

Published in Micro & Nano Letters
 Received on 20th January 2009
 Revised on 18th February 2009
 doi: 10.1049/mnl:20090007



Microfabrication of ultra-long reinforced silicon neural electrodes

M. Hajj-Hassan¹ V.P. Chodavarapu¹ S. Musallam^{1,2}

¹Department of Electrical and Computer Engineering, McGill University, 3480 University Street, Montreal, QC, Canada H3A 2A7

²Department of Physiology, McGill University, 3655 Promenade Sir William Osler, Montreal, QC, Canada H3G 1Y6
 E-mail: vamsy.chodavarapu@mcgill.ca

Abstract: The authors describe a simple dry-etch silicon microfabrication process to develop an array of electrodes with multiple recording sites suitable for neural recording applications. This new high-yield fabrication process uses commercially available ultra-thin silicon wafers as substrate material. A xenon difluoride system is used to etch the silicon substrate to form the electrode structures. The novel concept of structural reinforcement to produce elongated and reliable probe electrodes is introduced. The authors demonstrate recording silicon electrodes that can reach lengths longer than 10 mm having only 50 μm thicknesses and an 100 μm average width. This new microfabrication process illustrates a simple, cost-effective and mass-producible method for developing ultra-long silicon probes for deep brain implantation and neural recording.

1 Introduction

Brain-machine interfaces (BMIs) can assist paralysed patients by allowing them to operate computers or robots using their neural activity [1]. Integral to this endeavour is the development of brain implants that can be inserted into the surface or deep into the brain. The advancement of surface and bulk micromachining techniques played a significant role in standardising the production of brain implantable neural electrodes with very well-defined and sharp electrodes with precise placement of metallic neural electropotential recording sites [2]. Over the past several years, many research groups have employed microfabrication techniques to mass-produce silicon neural electrodes with high accuracy and repeatability [3–5]. Furthermore, there are research initiatives towards active neural probes with on-probe signal processing circuitry and/or integrated microactuators driving the electrode shank into the brain tissue while actively tracking the neuron movement [6–8].

The recording and processing of neural electropotential signals is required to understand how the brain processes information in response to controlling body functions. Motor and cognitive signals have both been shown to be viable signals for prosthetic applications. To date, many

neural prosthetic devices have been developed that used motor signals from the surface of the motor cortex to mainly derive hand trajectory signals [1, 9–11]. We plan to record cognitive signals from areas that are up to 10 mm below the surface of the brain [12]. Cognitive control signals for neural prosthetics is a relatively new concept that deals with tapping and understanding the messages of higher-order neurons involved in planning and motivation for movements such as reaching and grasping [12, 13]. These signals can be located in the posterior parietal reach region located medial to the intraparietal sulcus and the dorsal premotor cortex. These regions are located much deeper in the brain compared with the motor cortex, which provides the actual control signals for movements. Conventional electrodes, such as Utah Array [14] and Michigan Array [15], typically reach lengths less than 5 mm. Recently, Norlin *et al.* [16] have demonstrated 5-mm-long electrodes using deep reactive-ion-etching of silicon-on-insulator substrates. We set out to design and manufacture ultra-long probes that are small enough to minimise implantation damage to neuron networks but stiff enough to survive implantation.

Here, we describe the microfabrication process of neural electrodes that reach lengths longer than 10 mm while having a similar footprint as conventional electrodes. The process

uses commercial ultra-thin silicon substrates, and is cost-effective, repeatable and a high-yield method for neural electrode microfabrication. We propose the novel principle of reinforcing the electrodes in their more susceptible areas to improve their strength during implantation without increasing the dimensions of the probe. We describe the simulated and experimentally tested performance of the proposed ultra-long neural electrodes. We provide a comparative analysis of the fabricated neural electrodes between the reinforced and non-reinforced types. Specifically, we analyse the dynamics of structural probe reinforcement, which includes examining probe stiffness and critical buckling load to render probes suitable for gathering cognitive neural information.

2 Neural probe design and structural reinforcement

The developed neural electrode array consists of four tapered electrode probes constructed using a silicon substrate. Each electrode in the array is 10.5 mm in length and its structure is divided into three regions: (i) support base region, (ii) measuring region and (iii) piercing region, as shown in Fig. 1. The support base region measures 250 μm in length with a width of 350 μm at the base that rapidly reduces to a width of 150 μm , thus minimising brain tissue damage and displacement. The tapered wide base is designed to provide sufficient strength for each probe to survive during surgical implantation. The measuring region starts with a width of 150 μm at the base and ends up with 50 μm at the other end. The neural probe has an average width of 100 μm over the majority of the 10 mm length of the measuring region. The measuring region has three 20 μm \times 20 μm gold recording sites spaced 1 mm apart. Gold was selected for its biocompatibility and impedance characteristics. The measuring region is followed by the piercing region that

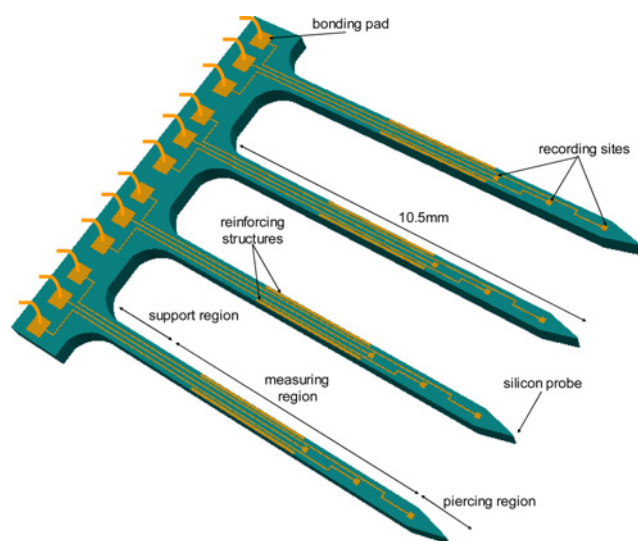


Figure 1 Design of the probe array carrying the recording sites, interconnects, reinforcing structures and bonding pads

forms the chisel-shaped tip of the probe with a length of 250 μm and is designed to be of 10 μm width at the end of the probe.

Many designs of elongated and ultra-long probes fail (crack or shatter) during implantation as they are unable to withstand the insertion axial forces, retraction forces and tension forces of the brain tissue [3]. These forces bring about bending and buckling of the probe. As the critical loads of a probe electrode are proportional to its thickness, the stability of a probe electrode can be improved by increasing its thickness. Such a design, however, will increase the damage of the brain tissue during the insertion phase of the probe. A better solution is obtained by keeping the thickness of the probe as small as possible and increasing the stability by introducing reinforcing structures. We notice that the probe stability can be improved by adding a stiff longitudinal reinforcing structure of suitable cross-section at the middle of the probe. The volume of such a reinforcement structure will be much smaller than the additional volume introduced by increasing the thickness of the probe.

To this end, we detail analytical studies to ascertain the reliability of the proposed ultra-long neural probe electrodes when they are subjected to significant stresses because of imperfect insertion into the brain and/or movement of the brain relative to the skull where the probe support is anchored. The main goal of the simulation is to predict the behaviour of the probe electrodes when they are subjected to an axial force. The axial force represents a critical parameter to develop reliable neural probe arrays as it determines the force at which the probe tip penetrates the brain tissue. In the case of an axially compressed probe, the maximum stress is located in the middle of the probe electrode. Therefore it is important to strengthen weaker areas located at the middle of the probe, which is the most susceptible region for breakage. Thus, the design of our new reinforced probe electrode is structurally similar to the conventional electrode but with additional metal layers added at the middle of the electrode.

The simulations shown in Fig. 2 were conducted using CoventorWare finite element analysis software from Coventor Inc. The mechanical behaviour of the electrode structures were studied using the mechanical solver MemMech, which is a part of CoventorWare. The model structure was meshed into parabolic tetrahedrons with an element size of 4 μm , which was selected so that the simulation converges towards a unique solution. For the simulation, a trajectory of axial force is applied horizontally at the cross-section face of the probe electrode. The recording sites, interconnections and bonding pads were not considered for simulations. The critical buckling load was obtained at the point where the maximum von Mises stresses, typically used to estimate yield and failure criteria in ductile materials, at weak regions of the probe reach 1 GPa, which is near the fracture stress limit for a thin silicon cantilever [17]. The critical loads for reinforced and

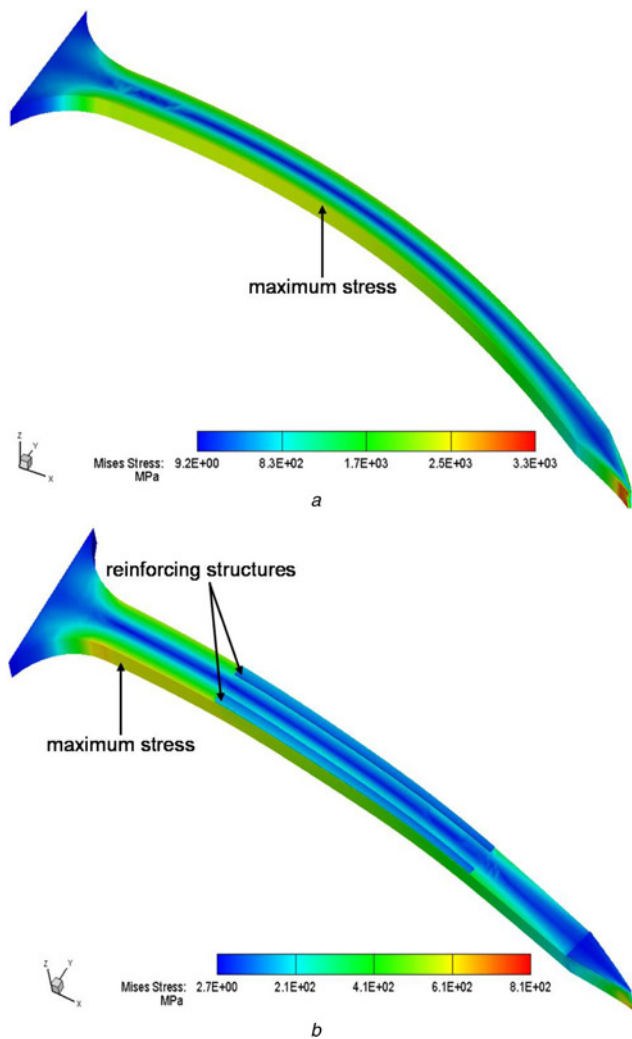


Figure 2 Behaviour of the 10.5-mm-long probe electrodes when they are subjected to axial horizontal force

- a Without reinforcement
b With reinforcement

non-reinforced electrodes from simulations were found to be 371 and 307 mN, respectively.

In the case of an axial force, the maximum stress is in the middle of the probe whereas an average stress value is present at the bottom of the probe. Fig. 2 shows a comparative stress analysis between the non-reinforced (Fig. 2a) and reinforced probe electrodes (Fig. 2b). We notice that adding a strip of metal along the side edges of the electrode increased its tensile strength by $\sim 10\%$ when compared with the classic electrode by pushing back the location of the maximum induced stress from the middle of the probe electrode to its base, which is typically wider than the rest of the probe. This enables the probe electrodes to be more resistant to the axial buckling force exerted by the brain tissue surface during implantation. We benefit from using the same $1\text{-}\mu\text{m}$ -thick titanium–gold metal layers used for forming the recording sites to reinforce the probe electrodes at the middle. The reinforcing structures are each 2 mm long and

placed exactly at the middle of the probe (or starting at 4 mm from the base and ending at 4 mm from the piercing tip end of the probe) with an average width of $40\ \mu\text{m}$ along their length.

3 Experimental results and discussion

Fig. 3 shows the cross-sectional view of the microfabrication process for the neural electrode array. The process starts with a $50\text{-}\mu\text{m}$ -thick, $4''$ -diameter double side polished, silicon wafer as substrate material. Firstly, metal layers of titanium (adhesion layer, 500 nm thick) and gold (conducting layer, 750 nm thick) were deposited on the silicon wafer (Fig. 3a). Secondly, the gold and titanium layers were photolithographically patterned and etched, with $1:2:10\ \text{I}_2:\text{KI}:\text{H}_2\text{O}$ and $20:1:1\ \text{H}_2\text{O}:\text{HF}:\text{H}_2\text{O}_2$, respectively, to define the recording pads, reinforcement layer and interconnects between the recording sites and bonding pads (Fig. 3b). Finally, the silicon substrate was patterned and etched using an isotropic xenon difluoride (XeF_2) etching system to form the electrode probes (Fig. 3c).

The XeF_2 etching technique was selected as it provides unique advantages compared with wet and other dry etch techniques; specifically related to its high etch rate ($1\text{--}3\ \mu\text{m}/\text{min}$ at room temperature), high aspect ratios, selectivity and simplicity [18]. The high selectivity of the XeF_2 etching to silicon can be used to make high-aspect structures with little or no degradation of the etch-stop or masking layer. Standard hard-baked photoresist can serve as an effective mask for deep and extended etches to obtain high aspect ratios. The use of a photoresist as a masking layer simplifies the fabrication process by obviating the need for deposition, patterning and etching of silicon dioxide or silicon nitride masking layers commonly used for other silicon dry or wet etch techniques. Fig. 4a is a photomicrograph for the fabricated electrode

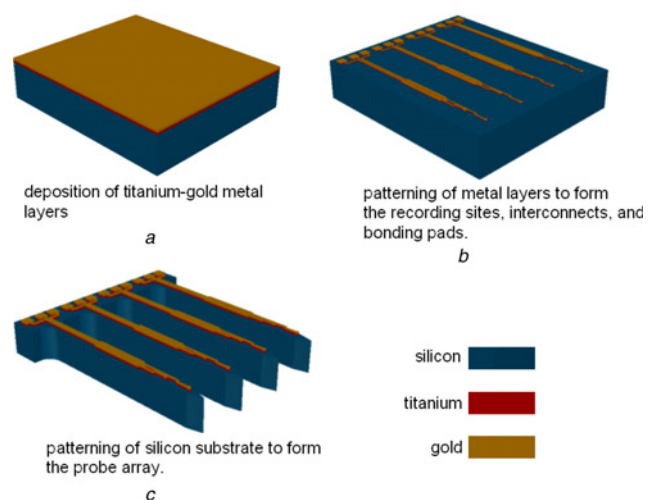


Figure 3 Schematic illustration of the steps involved in the fabrication process of the neural probe array. The figure is not to scale

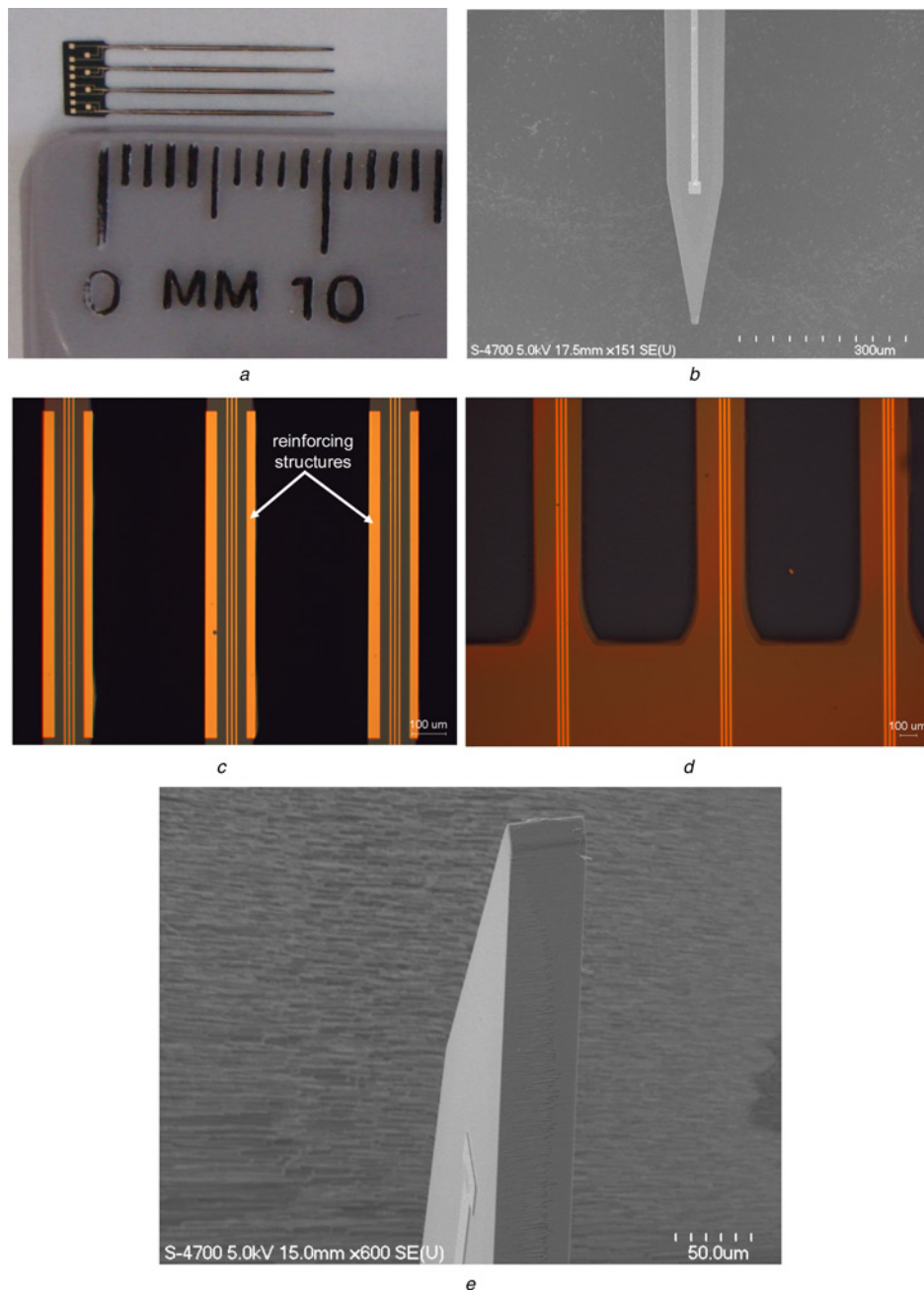


Figure 4 Microphotographs of the fabricated electrode array

- a* Picture of the fabricated electrode array
- b* Close-up view of the probe tip and the three $20\ \mu\text{m} \times 20\ \mu\text{m}$ recording sites
- c* Picture of the reinforcing structures
- d* View of the tapered base of the electrodes
- e* Cross-sectional view of the probe electrode

array. Fig. 4*b* is a scanning electron microscope (SEM) picture of the piercing and recording regions of a single electrode. It shows the well-defined, tapered and sharp tip of the electrode. It also shows the $20\ \mu\text{m} \times 20\ \mu\text{m}$ recording sites, which typically show an impedance of $1\ \text{M}\Omega$ at $1\ \text{kHz}$ required for neurophysiological measurements. The reinforcing structures located in the middle of the probes are shown in Fig. 4*c*. The interconnect lines shown are $10\ \mu\text{m}$ wide. Fig. 4*d* shows the tapered base of the probe electrode.

Fig. 4*e* shows the cross-sectional view of the probe electrode. The microelectrode array can be later encapsulated using Parylene-C as a biocompatible layer for surgical implantation with only the recording sites exposed to the neurons [19].

A successful penetration of the current array of neural electrodes into brain tissue is without breakage or excessive dimpling. In order to ensure the reliability of a silicon-based electrode, its design must be analysed and operational limits

defined. The pre-defined limit to which the electrodes can be stressed is often referred to as the buckling load, which represents the maximum allowable compressive loads that the probe electrodes are capable of withstanding without failure. The buckling load is determined more as a design parameter than a material property. We performed an experimental evaluation to determine the mechanical stability of the neural electrodes by determining the critical buckling load. In our application, the probe electrodes can be treated as cantilever beams that are fixed at one end and free to move at the other. When a critical load is applied, the buckling occurs in the plane perpendicular to the corresponding principal axis of inertia. As shown in Fig. 5, the critical loads were calculated by buckling the probe electrodes until the electrodes break and by measuring the maximum deflection, d_{\max} . We use (1) and (2) to calculate the critical stress σ_{cr} [20, 21]. The critical stress is then used to find the critical load, P_{cr} , of the beam under loading.

$$d_{\max} = \frac{\sigma_{\text{cr}} L^2}{6Et} \quad (1)$$

$$P_{\text{cr}} = \sigma_{\text{cr}} A \quad (2)$$

where E is the elastic modulus for silicon and is assumed to be 190 GPa, t is the probe electrode thickness and L is the length of the probe electrode [20, 21].

In order to measure the critical loads of the reinforced and non-reinforced probe electrodes, we fabricated an array of electrodes consisting of two non-reinforced electrodes and two reinforced electrodes in between. In this experiment, a horizontal loading setup was used for the buckling study. The test platform consists of an array of electrodes mounted and glued on a custom-designed printed circuit board (PCB) using an epoxy material to allow easy handling of the array during the test procedure as shown in Fig. 6a. The PCB is then mounted on a motion controller to allow a slow advancement of the probe electrodes in small and accurate steps. The electrodes were advanced to touch a hard plastic surface. As the electrodes moved forward and pressed against the hard surface, the deflection of the electrodes increased. Fig. 6b provides a visual explanation of the buckling experiment. The values of the maximum deflections d_{\max} of the reinforced and non-reinforced electrodes were measured from Fig. 6b using a microscope and a micrometre grid and are found to be 1280 and 1100 μm , respectively. Based on the stress deflection equations described previously, the critical

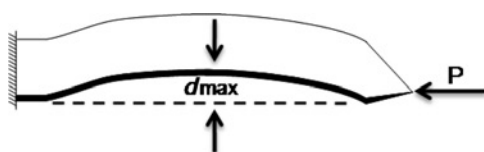


Figure 5 Diagram of a single probe electrode under buckling deflection condition

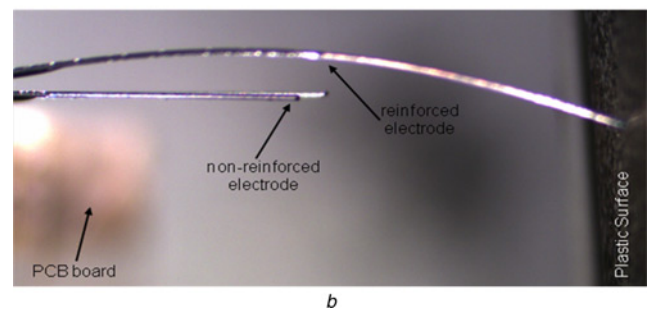
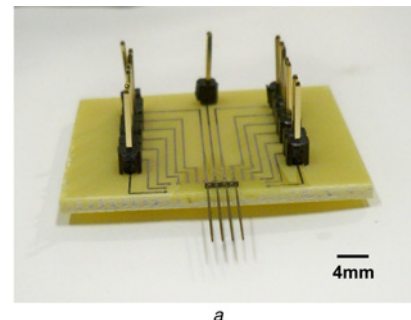


Figure 6 Buckling testing of probe electrodes when pressed against a hard plastic surface

stresses of the reinforced and non-reinforced probe electrodes as they are pressed against the hard surface were calculated to be 364.8 and 313.5 mN, respectively. The measured critical buckling loads are in good agreement with the simulated results.

4 Conclusions

We report the first demonstrated neural microelectrode array fabricated using standard ultra-thin silicon wafers as substrates and a XeF_2 etching system. The microfabrication process provides a rapid, cost-effective and high-yield platform to manufacture neural electrodes required to gather cognitive neural information. We also introduce a novel concept of structural reinforcement for neural electrodes to improve their tensile strength for deep brain implantation studies. The reinforcement increases the stability of the electrodes by augmenting the critical buckling load by approximately 50 mN. The resulting neural electrodes reach comparatively elongated lengths of 10.5 mm having only a 50 μm thickness. The developed electrodes possess well-defined structural features with smooth surfaces.

5 Acknowledgments

This work was financially supported by the Natural Sciences and Engineering Research Council (NSERC) and Canadian Institutes of Health Research (CIHR). We would like to acknowledge the assistance of the McGill's Nanotools and Microfabrication Laboratory in preparing the described samples.

6 References

- [1] TAYLOR D.M., TILLERY S.I.H., SCHWARTZ A.B.: 'Direct cortical control of 3D neuroprosthetic devices', *Science*, 2002, **296**, pp. 1829–1832
- [2] NAJAFI K.: 'Micromachined systems for neurophysiological applications', in 'Handbook of microlithography, micromachining and microfabrication', Volume II: Micromachining and microfabrication' (SPIE Press Monograph, London, 1997)
- [3] HAJJ-HASSAN M., CHODAVARAPU V., MUSALLAM S.: 'NeuroMEMS: neural probe microtechnologies', *Sensors*, 2008, **8**, pp. 6704–6726
- [4] WISE K.D., NAJAFI K.: 'Microfabrication techniques for integrated sensors and microsystems', *Science*, 1991, **254**, pp. 1335–1342
- [5] PEARCE T.M., WILLIAMS J.C.: 'Microtechnology: meet neurobiology', *Lab. Chip.*, 2007, **7**, pp. 30–40
- [6] JI J., NAJAFI K., WISE K.D.: 'A scaled electronically-configurable multichannel recording array', *Sens. Actuators A – Phys.*, 1990, **22**, pp. 589–591
- [7] OLSSON R.H., BUHL D.L., SIROTA A.M., BUZSAKI G., WISE K.D.: 'Band-tunable and multiplexed integrated circuits for simultaneous recording and stimulation with microelectrode arrays', *IEEE Trans. Biomed. Eng.*, 2005, **52**, pp. 1303–1311
- [8] MUTHUSWAMY J., OKANDAN M., JAIN T., GILLETTI A.: 'Electrostatic microactuators for precise positioning of neural microelectrodes', *IEEE Trans. Biomed. Eng.*, 2005, **52**, pp. 1748–1755
- [9] DONOGHUE J.P.: 'Connecting cortex to machines: recent advances in brain interfaces', *Nat. Neurosci.*, 2002, **5**, pp. 1085–1088
- [10] SERRUYA M.D., HATSOPOULOS N.G., PANINSKI L., FELLOWS M.R., DONOGHUE J.P.: 'Instant neural control of a movement signal', *Nature*, 2002, **416**, pp. 141–142
- [11] CARMENA J.M., LEBEDEV M.A., CRIST R.E., ET AL.: 'Learning to control a brain–machine interface for reaching and grasping by primates', *PLoS Biol.*, 2003, **1**, pp. 193–208
- [12] MUSALLAM S., CORNEIL B.D., GREGER B., SCHERBERGER H., ANDERSEN R.A.: 'Cognitive control signals for neural prosthetics', *Science*, 2004, **305**, pp. 258–262
- [13] PESARAN B., MUSALLAM S., ANDERSEN R.A.: 'Cognitive neural prosthetics', *Curr. Biol.*, 2006, **16**, R77–R80
- [14] ROUSCHE P.J., NORMANN R.A.: 'Chronic recording capability of the Utah Intracortical Electrode Array in cat sensory cortex', *J. Neurosci. Meth.*, 1998, **82**, pp. 1–15
- [15] WISE K.D., ANDERSON D.J., HETKE J.F., KIPKE D.R., NAJAFI K.: 'Wireless implantable microsystems: high-density electronic interfaces to the nervous system', *Proc. IEEE*, 2004, **92**, pp. 76–97
- [16] NORLIN P., KINDLUNDH M., MOUROUX A., YOSHIDA K., HOFMANN U.G.: 'A 32-site neural recording probe fabricated by DRIE of SOI substrates', *J. Microelectromech. Syst.*, 2002, **12**, pp. 414–419
- [17] WILSON C.J., BECK P.A.: 'Fracture testing of bulk silicon microcantilever beams subjected to a side load', *J. Microelectromech. Syst.*, 1996, **5**, pp. 142–150
- [18] HOFFMAN E., WARNEKE B., KRUGLICK E., WEIGOLD J., PISTER K.S.J.: '3D Structures with piezoresistive sensors in standard CMOS'. Proc. IEEE Micro Electro Mechanical Systems Conf., Amsterdam, The Netherlands, 1995, pp. 228–293
- [19] MUSALLAM S., MARTIN J.B., PHILIP R.T., RICHARD A.A.: 'A floating metal microelectrode array for chronic implantation', *J. Neurosci. Meth.*, 2007, **160**, pp. 122–127
- [20] PEARSON G.L., READ W.T. JR., FELDMAN W.L.: 'Deformation and fracture of small silicon crystals', *Acta Metall.*, 1957, **5**, pp. 181–191
- [21] NAJAFI K., HETKE J.F.: 'Strength characterization of silicon microprobes in neurophysiological tissues', *IEEE Trans. Biomed. Eng.*, 1990, **37**, pp. 474–481